Biosensors and Bioelectronics 23 (2008) 1869–1873

Contents lists available at ScienceDirect

Biosensors and Bioelectronics

journal homepage: www.elsevier.com/locate/bios

A novel nitrite biosensor based on the direct electron transfer of hemoglobin immobilized on CdS hollow nanospheres

Zhihui Dai*, Hongyan Bai, Mei Hong, Yinyan Zhu, Jianchun Bao, Jian Shen*

Jiangsu Key Laboratory of Biofunctional Materials, College of Chemistry and Environmental Science, Nanjing Normal University, Nanjing 210097, PR China

ARTICLE INFO

Article history:
Received 1 February 2008
Accepted 5 March 2008
Available online 14 March 2008

Keywords:
Nitrite
Biosensor
Direct electron transfer
Hemoglobin
CdS hollow nanospheres

ABSTRACT

A novel nitrite biosensor based on the direct electron transfer of hemoglobin (Hb) immobilized on CdS hollow nanospheres (HS-CdS) modified glassy carbon electrode was constructed. The direct electron transfer of Hb showed a pair of redox peaks with a formal potential of −286 mV (vs. SCE) in 0.1 M pH 7.0 phosphate buffer solution. It was a surface-controlled electrode process involving a single proton transfer coupled with a reversible one-electron transfer for each heme group of Hb. HS-CdS had a large specific surface area and good biocompatibility and had a better electrochemical response than that of solid spherical CdS. The immobilized Hb on HS-CdS displayed an excellent response to NO_2^- with one irreversible electrode process for NO reduction. Under optimal conditions, the biosensor could be used for the determination of NO_2^- with a linear range from 0.3 to 182 μM and a detection limit of 0.08 μM at 3σ based on the irreversible reduction of NO. HS-CdS provided a good matrix for protein immobilization and had a promising application in constructing sensors.

1. Introduction

Nitrite is an important precursor in the formation of *N*-nitrosamines, many of which have been shown as potent carcinogens in human bodies (Lijinsky and Epstein, 1970; Mirvish, 1995). It also exists widely in the environment, beverages and food products as a preservative (Davis and Campton, 2000). As an alarming pollutant to the environment and human health (Moorcroft et al., 2001), various techniques have been developed to determine nitrite, such as spectrophotometry (Kuznetsov and Zemyatova, 2007; Takiguchi et al., 2006), chromatography (Prusisz et al., 2006; Niedzielski et al., 2006), capillary electrophoresis (Miyado et al., 2007), chemiluminescence (Lagalante et al., 2007) and electrochemistry (Strehlitz et al., 1996; Larsen et al., 2000; Liu and Ju, 2003; Dai et al., 2004). Especially, the potential low cost and portability of electroanalytical devices provide a number of attractive options. The sensors based on the electrochemical methods mentioned above are favorable for nitrite determination with high sensitivity, relatively good selectivity and fast response. However, there are two disadvantages. It is difficult to get them sufficiently stable upon exposing them directly to real samples due to fouling of the electrode surface (Larsen et al., 2000), denaturation of enzymes, or slow removal of modifiers from the sensor's surface (O'Shea et al., 1992). Another problem is the commercial unavailability of some modifiers which limits their extensive application.

Nitrite can be first reduced to NO according to the following reaction:

$$NO_2^- + 2H^+ + e^- \rightarrow NO + H_2O$$

NO has recently been recognized as a natural metabolite and has been associated with many physiological and pathological processes (Palmer et al., 1987; Stamler, 1994). It has a high affinity with hemoglobin (Hb) by binding to Fe(II) in Hb (Gow and Stamler, 1998). The electrochemical determination of NO as well as its interaction with Hb has attracted considerable attention (Maskus et al., 1996; Gow and Stamler, 1998; Rakesh, 2000; Andrea et al., 2001; Grzelak et al., 2001). Also, the direct electron transfer between Hb and electrodes and electrocatalysis to nitrite has been achieved by immobilizing Hb on carbon nanotube (Liu et al., 2007), zeolite particles (Xie et al., 2007), mesoporous silica (Dai et al., 2004) and clay (Zhou et al., 2002). These materials provided biomembrane-like microenvironments and facilitated direct, chemically reversible electron exchange between Hb and electrodes, and eliminated the need of mediators. They also had good electrocatalytic responses to nitrite.

It is noted that nano-sized CdS has recently been used in immobilizing Hb and the direct electron transfer has been obtained (Zhou et al., 2005). However, it was used to construct a H_2O_2 biosensor

* Corresponding authors. Tel.: +86 25 83598031.
E-mail addresses: daizhihuii@njnu.edu.cn (Z. Dai), jshen@njnu.edu.cn (J. Shen).

0956-5663/$ – see front matter © 2008 Elsevier B.V. All rights reserved.
doi:10.1016/j.bios.2008.03.002

and the used CdS was of the solid spheres. The biosensor of nitrite based on CdS has not been reported yet. In this work, CdS hollow nanospheres (HS-CdS) are firstly used to study the direct electrochemical behavior of Hb and the construction of nitrite biosensor. The presence of HS-CdS increases the response current of immobilized Hb and the modified electrode shows a good electrochemical response to nitrite with one irreversible electrode process for NO reduction, revealing HS-CdS has the potential application in constructing biosensors.

2. Experimental

2.1. Reagents and materials

Hb (bovine blood) was obtained from Sigma and used without further purification. Other reagents were of analytical reagent grade. All solutions were prepared with doubly distilled water. Phosphate buffer solutions (PBS, 0.1 M) with various pH values were prepared by mixing stock standard solutions of K_2HPO_4 and KH_2PO_4 and adjusting the pH with H_3PO_4 or NaOH.

2.2. Electrode preparation

HS-CdS spheres and CdS solid spheres (SS-CdS) with the diameter in the range of 15–30 nm were prepared following a recipe by our previous work (Dai et al., 2007). The preparation procedures of the modified electrodes were as follows: 30 mg of hollow or solid CdS nanospheres were dispersed into 10-mL 0.1 mM Hb (in pH 7.0 PBS) solution. The mixture was stirred for 3 h to obtain a suspension. 100 μL of the obtained suspension was then mixed with 5 μL of 10% Nafion solution to produce Hb/CdS/Nafion colloid solution that was used for the following work. The glassy carbon electrodes (GCE, 3 mm in diameter) were polished to a mirror-like finish with 1.0, 0.3 and 0.05 μm alumina slurry (Beuhler) followed by rinsing thoroughly with doubly distilled water. The electrodes were successively sonicated in 1:1 nitric acid, acetone and doubly distilled water, and then allowed to dry at room temperature. The real area of the pretreated GCE was 0.092 cm^2, which was determined from the slope of the plot of the anodic peak current of 1.0 mM $K_3[Fe(CN)_6]$ in 0.1 M KCl at the GCE versus the square root of scan rate. 3 μL Hb/CdS/Nafion colloidal solution was dropped on the pretreated GCE surface and allowed to dry under ambient condition for 3 h. After the modified electrode was rinsed with doubly distilled water twice or thrice, Hb/CdS modified GCE was obtained. When not in use the electrode was stored in 0.1 M pH 7.0 PBS at 4 °C.

2.3. Measurements

The morphology and particle size of the samples were characterized by JEM-200CX transmission electron microscopy (TEM). UV–vis absorption spectrum was obtained on a Varian Cary 5000 spectrophotometer. Circular dichroic (CD) measurements were made on JASCO Model J-810 dichrograph (Japan Spectroscopic Co. Ltd., Tokyo, Japan) at room temperature in an 1-cm quartz cuvette. The measurement of surface area of the sample was performed using ASAP 2020 Micromeritics. AC impedance experiments were carried out with the PGSTAT30/FRA2 system (Autolab, The Netherlands).

Cyclic voltammetric and amperometric measurements were performed on CHI 660 electrochemical workstation (CH Instruments, USA). All electrochemical experiments were carried out in a cell containing 5.0-mL 0.1 M PBS at room temperature (25 ± 2 °C) and using a platinum wire as auxiliary, a saturated calomel electrode as reference and the modified GCEs as working electrodes. All solutions were deoxygenated by bubbling highly pure nitrogen for at least 20 min and maintained under nitrogen atmosphere during measurements. The amperometric experiments were carried out by applying potential of −850 mV for nitrite on a stirred cell at 25 ± 2 °C. The sensor responses were measured as the difference between total and residual currents.

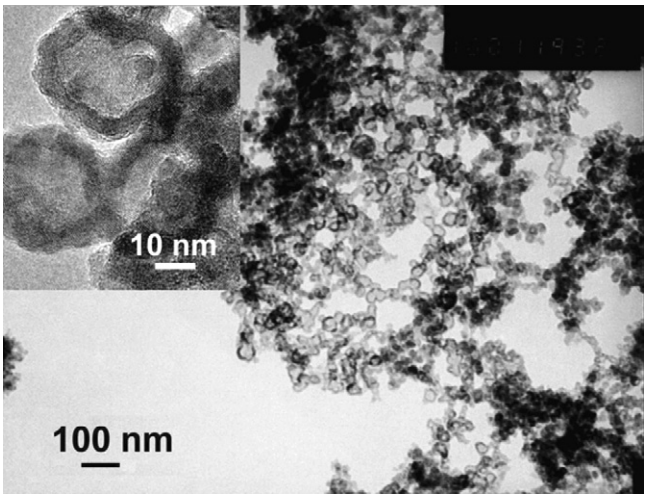

Fig. 1. TEM images of HS-CdS at lower and higher (inset) magnification.

3. Results and discussion

3.1. The morphology of HS-CdS

The TEM image of the prepared CdS particles is shown in Fig. 1. From the image, we can see the pale color regions in the central parts in contrast to dark edges, implying a hollow spherical structure. Moreover, the contrast between the center and edge in the TEM images of one sphere remains unchangeable when the sample grid is rotated by different degrees, proving their hollow structures. The average diameter of the hollow spheres is about 25 nm with mainly ranging from 15 to 35 nm. The shell thickness of 5 nm can be obtained from the inset in Fig. 1 which shows the TEM image of HS-CdS at higher magnification.

3.2. The interaction between Hb and HS-CdS

Fig. 2A shows the UV–vis spectra of Hb (a) and Hb/HS-CdS (b), respectively. There is no absorption band of HS-CdS (figure not shown). Comparing two curves, the absorption band of Hb/HS-CdS is located at 406 nm, which is at the same position as that for the free Hb (not adsorbed), suggesting that no significant denaturation occurs (George and Hanania, 1953; Nassar et al., 1995) and Hb is immobilized on HS-CdS and maintains its native structure. Such immobilizing process does not destroy the structure of Hb and does not change the fundamental microenvironment of Hb.

Since CD spectroscopy is able to give an insight into the structure and the conformation of the proteins/enzymes (Degli Esposti et al., 1987), CD spectroscopy is used to further characterize the structural integrity of Hb immobilized on HS-CdS. Fig. 2B shows the CD spectra of Hb and Hb/HS-CdS. The CD spectrum of Hb exhibits two negative peaks at ca. 208 and 223 nm (curve a in Fig. 2B), respectively, which is similar to those of the other heme containing proteins (Hanlon et al., 2000). The positions of CD spectrum of Hb/HS-CdS (curve b in Fig. 2B) are almost the same as those in curve a in Fig. 2B. The similarities between the CD spectra of curves a and b in Fig. 2B indicate that the structure and the conformation of Hb remain after being immobilized on HS-CdS.

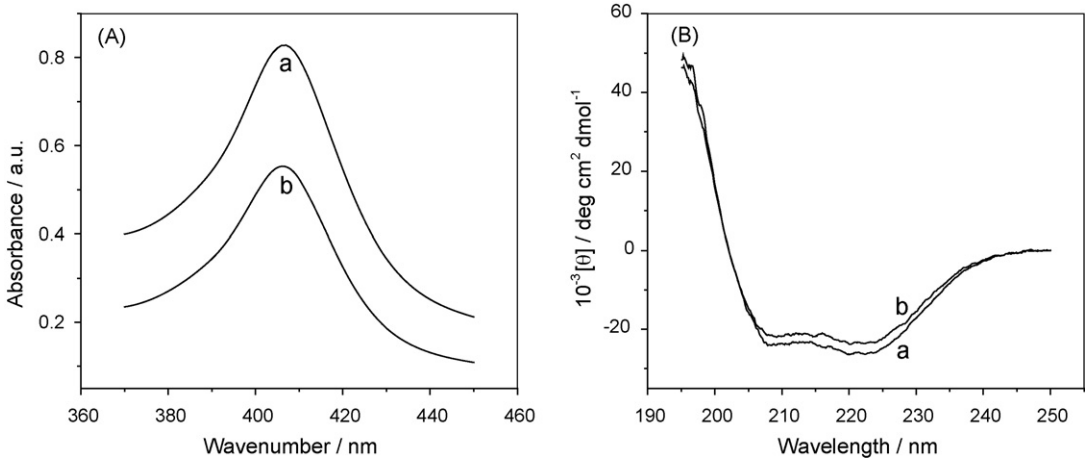

Fig. 2. UV–vis spectra (A) and CD spectra (B) of Hb (a) and Hb/HS-CdS (b).

The electrochemical impedance spectra (EIS) of the modified electrodes were shown in Fig. 3. The impedigrams revealed that compared to the bare GCE (curve a in Fig. 3), the impedance increased upon addition of HS-CdS to the surface of GCE (curve b in Fig. 3). An obvious increase in impedance was also observed upon addition of Hb to the surface of GCE (curve c in Fig. 3). HS-CdS with Hb, however, decreased the measured impedance of the modified GCE (curve d in Fig. 3) which indicated that the presence of HS-CdS with Hb could decrease the interfacial resistance to electron transfer over Hb alone.

3.3. Direct electrochemistry of Hb/HS-CdS modified electrode

The cyclic voltammetry (CV) was performed to observe whether the protein retained its electrochemical activity after the immobilizing procedure. Fig. 4 shows the cyclic voltammograms of different electrodes in 0.1 M pH 7.0 PBS at 100 mV s^{-1}. No peak was observed at bare (curve a in Fig. 4) and HS-CdS (curve b in Fig. 4) modified GCEs, respectively, which showed HS-CdS was electroinactive in the potential window. The Hb modified GCE also showed the response of Hb (curve c in Fig. 4), but there was only an irreversible reduction peak and the response was smaller than that of the Hb/HS-CdS modified GCE (curve d in Fig. 4). The Hb/HS-CdS modified GCE exhibited a couple of stable redox peaks that were attributed to the redox of immobilized Hb with the peak-to-peak separation of 100 mV. The value of $E^{0\prime}$ (vs. SCE) was −286 mV, which was close to the value of Hb in solution (Lu and Dong, 1990). For comparison, Hb/SS-CdS modified GCE has been carried out (curve e in Fig. 4). It revealed that the reversibility and redox response from Hb/HS-CdS modified GCE were better than those from Hb/SS-CdS modified GCE. The response was 2.2 times larger than that of Hb/SS-CdS modified GCE, indicating HS-CdS played an important role in maintaining the biological activity of Hb and facilitating the electron exchange between the Hb and the electrode surface.

The difference of redox response between the solid and the hollow spheres CdS might result from the difference of the Brunauer–Emmett–Teller (BET) surface areas. BET surface area of the HS-CdS calculated from N_2 adsorption isotherm is about 98 m^2 g^{-1} (14,151 m^2 mol^{-1}), which is much larger than the value of about 50 m^2 g^{-1} (7220 m^2 mol^{-1}) calculated for the surface area of solid spheres. This result is in agreement with the case of hollow palladium spheres (Kim et al., 2002).

With an increasing scan rate, the redox peak currents increased. The peak currents were proportional to the scan rates, indicating a surface-controlled electrode process. An average surface coverage of Hb was obtained from the peak areas of cyclic voltammograms at 50, 100 and 150 mV s^{-1} to be $(1.7 \pm 0.5) \times 10^{-10}$ mol cm^{-2}.

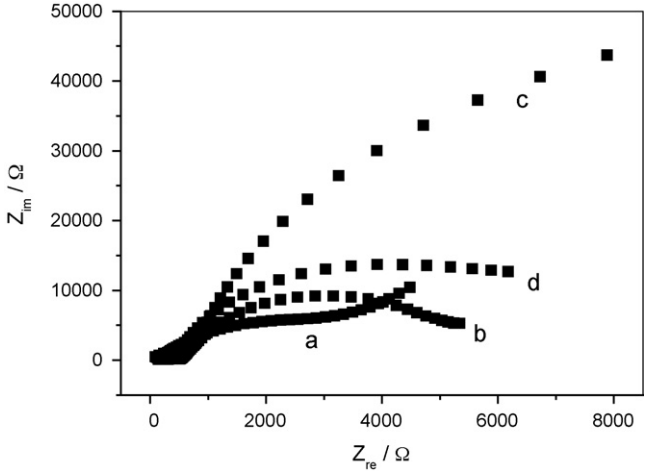

Fig. 3. Electrochemical impedance spectra recorded at bare (a), HS-CdS (b), Hb (c) and Hb/HS-CdS (d) modified GCEs in 0.1 M pH 7.0 PBS containing 1 mM K[Fe(CN)$_6$]. Frequency range: 1–10^6 Hz.

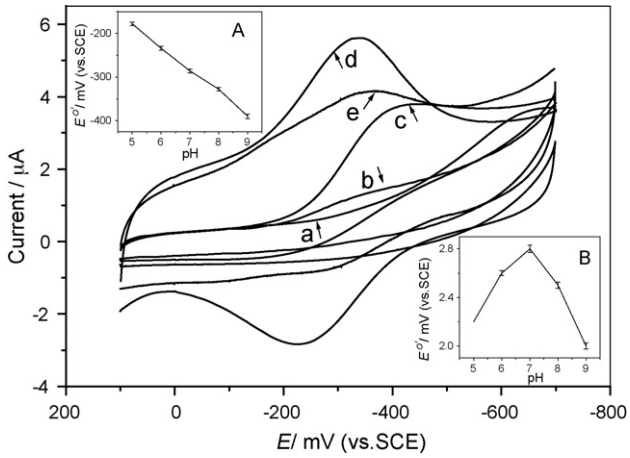

Fig. 4. Cyclic voltammograms of bare (a), HS-CdS (b), Hb (c), Hb/HS-CdS (d) and Hb/SS-CdS (e) modified GCEs in 0.1 M pH 7.0 PBS at 100 mV s^{-1}. Inset: plots of formal potentials (A) and peak currents (B) vs. pH of Hb/HS-CdS modified GCE.

CVs of Hb in Hb/HS-CdS modified GCE showed a strong dependence on solution pH. All changes in CV peak potentials and currents caused by solution pH were reversible in the range from 5.0 to 9.0; that is, the same CV could be obtained if the electrode was transferred back to its original solution. An increase of solution pH resulted in negative shifts in both cathodic and anodic peak potentials. The plot of the formal potential versus pH (from 5.0 to 9.0) produced a line with a slope of $-(51.5 \pm 2.2)$ mV/pH (inset A in Fig. 4), which was close to but smaller than the expected value of −58.0 mV/pH. It indicated the electron transfer process was close to a single proton transfer coupled with a reversible single electron transfer and was influenced by the ionic strength of the electrolyte. Altering the pH of the supporting electrolyte with either H_3PO_4 or NaOH would cause changes in the ionic strength of the electrolyte. The value of the slope was the synergetic effects by both pH and ionic strength. Inset B in Fig. 4 shows the relationship between the peak currents of the Hb/HS-CdS modified GCE and pH values. Obviously, the maximum current response occurred at pH 7.0.

3.4. Electrocatalysis reduction of NO_2^- with Hb/HS-CdS modified GCE

Fig. 5 shows the cyclic voltammograms of Hb/HS-CdS modified GCE in 0.1 M pH 7.0 PBS containing 0, 20 and 30 μM $NaNO_2$ at 100 mV s^{-1}. Upon addition of $NaNO_2$, a new irreversible reduction wave occurs at about −850 mV, which is attributed to the reduction of NO that came from the reduction of nitrite. At a more negative potential, NO can further be reduced irreversibly to N_2O, and then to NH_2OH or NH_3. Furthermore, the reduction current increases with an increase of NO_2^- concentration. For comparison, we performed the experiment by using a HS-CdS modified GCE (without Hb) in 0.1 M pH 7.0 PBS containing 20 μM $NaNO_2$ at 100 mV s^{-1} (inset in Fig. 5). It showed that no irreversible reduction wave occurred at about −850 mV which indicated that the irreversible reduction wave was not a result of the new HS-CdS.

Fig. 6 shows the amperometric response of the Hb/HS-CdS and Hb/SS-CdS modified GCEs with successive additions of $NaNO_2$ to 0.1 M pH 7.0 PBS at an applied potential of −850 mV, respectively. The current is produced from the reduction of NO that came from the reduction of nitrite (Barley et al., 1986; Younathan et al., 1992). Upon addition of an aliquot of NO_2^- to the buffer, the reduction current increases steeply, indicating a fast reduction rate. With

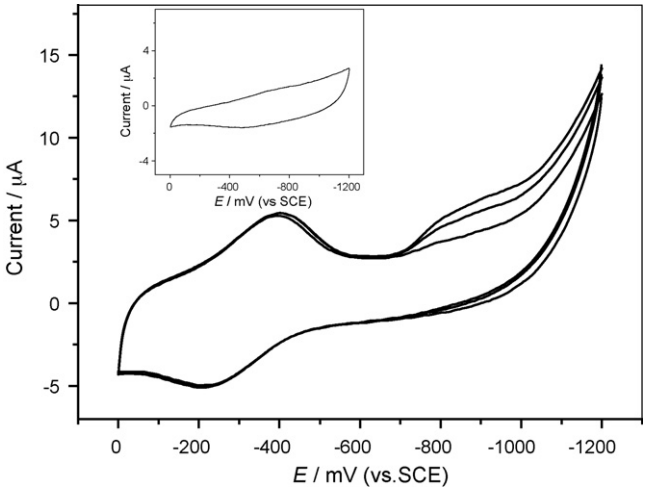

Fig. 5. Cyclic voltammograms of the Hb/HS-CdS modified GCE in pH 7.0 PBS containing 0, 20 and 30 μM $NaNO_2$ (from bottom to top) measured at 100 mV s^{-1}. Inset: cyclic voltammograms of the HS-CdS modified GCE in pH 7.0 PBS containing 20 μM $NaNO_2$ measured at 100 mV s^{-1}.

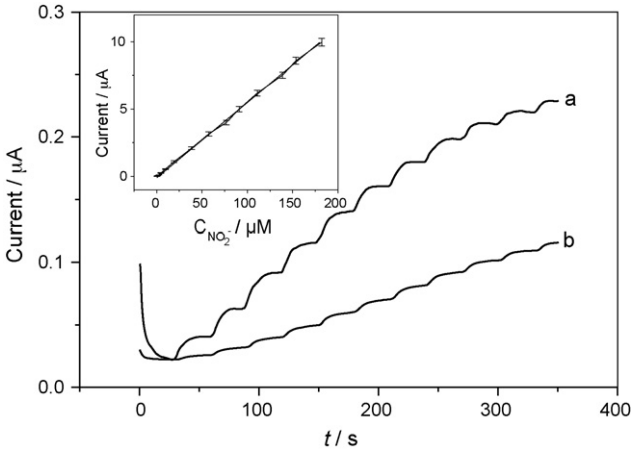

Fig. 6. Amperometric responses of the Hb/HS-CdS (a) and Hb/SS-CdS (b) modified GCEs at −850 mV upon successive additions of 5-μL 0.3 mM $NaNO_2$ to 5.0 mL pH 7.0 PBS. Inset: linear relation between the amperometric response and NO_2^- concentration.

an increase of NO_2^- concentration, the amperometric response increases. It is noted that the electrocatalytic current of Hb/HS-CdS modified GCE was about 2.5 times larger than that of Hb/SS-CdS modified GCE. Inset in Fig. 6 shows the calibration curve of the Hb/HS-CdS modified GCE to NO_2^-. The linear response range of the sensor to NO_2^- concentration is from 0.3 to 182 μM with a correlation coefficient of 0.9999 ($n = 19$) which is much wider than 0.2 to 3.8 μM for Hb immobilized on hexagonal mesoporous silica (Dai et al., 2004). The average relative standard deviation (R.S.D.) of the plots is 4.1%. The detection limit of 0.08 μM is obtained at a signal-to-noise ratio of 3 which is much lower than that reported for the detection limit of 34.0 μM NO_2^- for Hb immobilized in titania sol–gel film (Zhao et al., 2006) and similar to 0.06 μM for Hb immobilized in Au colloid (Liu and Ju, 2003). At 40 μM NO_2^- concentration the mean steady-state current for six determinations is 2.2 μA with an R.S.D. of 3.8%. At NO_2^- concentrations higher than 182 μM, the calibration curve shows a platform.

3.5. Stability and reproducibility of the NO_2^- sensors

The fabrication reproducibility of six electrodes, made independently, showed an acceptable reproducibility with a R.S.D. of 4.2% for the current determined at a NO_2^- concentration of 40 μM. Thus, HS-CdS were very efficient for retaining the electrocatalytic activity of Hb and preventing it from leaking out of the sensor.

In addition to good reproducibility, HS-CdS membrane imparted NO_2^- biosensors a good long-term stability. The direct electrochemistry of the Hb/HS-CdS modified GCE could retain the constant current values upon the continuous cyclic sweep over the potential range from −0.7 to +0.1 V at 100 mV s^{-1}. The immobilized Hb only lost 9.5% of its initial activity after more than 300 successive measurements. The storage stabilities of NO_2^- biosensors stored in 0.1 M pH 7.0 PBS or in air at 4 °C were examined by checking periodically their relative response currents (the ratios of the catalytic currents detected at different times to the initial current value) in 0.1 M pH 7.0 PBS containing 40 μM NO_2^-. The sensors could retain 95% of activity to NO_2^- within a storage period of 1 month in 0.1 M pH 7.0 PBS at 4 °C, while only 80% of activity to NO_2^- was retained when stored in air at 4 °C, respectively. After a storage period of 3 months in 0.1 M pH 7.0 PBS at 4 °C the biosensor showed an 8% loss of activity for NO_2^-. Thus, the biosensors were stored in 0.1 M pH 7.0 PBS at 4 °C when not in use.

4. Conclusion

Hemoglobin can be effectively immobilized in HS-CdS matrix. The Hb/HS-CdS modified GCE shows a fast direct electron transfer of Hb. The HS-CdS nanostructure provides a microenvironment around the protein to retain the enzymatic bioactivity. The immobilized Hb displays a good electrocatalytic response to nitrite. The sensor shows a wide linear range, low detection limit, good reproducibility and stability. Such a novel HS-CdS provides an efficient strategy and a new promising platform for the study of electron transfer of proteins and the development of biosensors.

Acknowledgements

This work was supported by the National Natural Science Foundation of China (Nos. 20505010 and 20473038), Science and Technology Development Center of National Ministry of Education of China (No. 20050319010), Major Base Research of National Science and Technology Department of China (No. 2005CCA00400), and Hi-Tech Research and Development Program of China (863 Program) (No. 2006AA032Z445).

References

Andrea, C., Miklos, G., 2001. Anal. Chem. 73, 3965–3974.
Barley, M.H., Takcuchi, K.J., Meyer, T.J., 1986. J. Am. Chem. Soc. 108, 5876–5885.
Dai, Z.H., Liu, S.Q., Ju, H.X., Chen, H.Y., 2004. Biosens. Bioelectron. 19, 861–867.
Dai, Z.H., Zhang, J., Huang, X.H., Bao, J.C., Mo, X.Y., 2007. J. Mater. Chem. 17, 1087–1093.
Davis, J., Campton, R.G., 2000. Anal. Chim. Acta 404, 241–247.
Degli Esposti, M., Ballester, F., Solaini, G., Lenaz, G., 1987. J. Biochem. 241, 285–290.
George, P., Hanania, G., 1953. Biochem. J. 55, 236–243.
Gow, A.J., Stamler, J.S., 1998. Nature 391, 169–173.
Grzelak, A., Balcerczyk, A., Mateja, A., Bartosz, G., 2001. Biochim. Biophys. Acta 1528, 97–100.
Hanlon, M.R., Begum, R.R., Newbold, R.J., Whitford, D., Wallace, B.A., 2000. J. Biochem. 352, 117–124.
Kim, S.W., Kim, M., Lee, W.Y., Hyeon, T., 2002. J. Am. Chem. Soc. 124, 7642–7643.
Kuznetsov, V.V., Zemyatova, S.V., 2007. J. Anal. Chem. 62, 637–644.
Lagalante, A., Greenbacker, P., 2007. Anal. Chim. Acta 590, 151–158.
Larsen, L.H., Damgaard, L.R., Kjaer, T., Stenstrom, T., Lynggard-Jensen, A., Revsbech, P., 2000. Water Res. 34, 2458–2463.
Lijinsky, W., Epstein, S.S., 1970. Nature 225, 21–23.
Liu, S.Q., Ju, H.X., 2003. Analyst 128, 1420–1424.
Liu, S.Q., Lin, B.P., Yang, X.D., Zhang, Q.Q., 2007. J. Phys. Chem. B 111, 1182–1188.
Lu, Z., Dong, S., 1990. Electrochim. Acta 35, 1139–1143.
Maskus, M., Pariente, F., Wu, Q., Toffanin, A., Shapleigh, J.P., Abruña, H.D., 1996. Anal. Chem. 68, 3128–3134.
Mirvish, S.S., 1995. Cancer Lett. 93, 17–48.
Miyado, T., Tanaka, Y., Nagai, H., Takeda, S., Saito, K., Fukushi, K., Yoshida, Y., Nadzhafova, O., Etienne, M., Walcarius, A., 2007. Electro. Commun. 9, 1189–1195.
Moorcroft, M.J., Davis, J., Compton, R.G., 2001. Talanta 54, 785–803.
Nassar, A.-E.F., Willis, W.S., Rusling, J.F., 1995. Anal. Chem. 67, 2386–2392.
Niedzielski, P., Kurzyca, I., Siepak, J., 2006. Anal. Chim. Acta 577, 220–224.
O'Shea, T.J., Leech, D., Smyth, M.R., Vos, J.G., 1992. Talanta 39, 443–447.
Palmer, J., Ferrige, A.G., Moncada, S., 1987. Nature 327, 524–526.
Prusisz, B., Jaskiewicz, L., Pohl, P., 2006. Microchim. Acta 156, 219–223.
Rakesh, P.P., 2000. Free Radic. Biol. Med. 28, 1518–1525.
Stamler, J.S., 1994. Cell 78, 931–936.
Strehlitz, B., Grundig, B., Schumacher, W., Kroneck, P.M.H., Vorlop, K.D., Kotte, H., 1996. Anal. Chem. 68, 807–816.
Takiguchi, H., Tsubata, A., Miyata, M., Odake, T., Hotta, H., Umemura, T., Tsunoda, K., 2006. Anal. Sci. 22, 1017–1019.
Xie, Y., Liu, H.Y., Hu, N.F., 2007. Bioelectrochemistry 70, 311–319.
Younathan, J.N., Wood, K.S., Meyer, T.J., 1992. Inorg. Chem. 31, 3280–3285.
Zhao, S., Zhang, K., Sun, Y.Y., Sun, C.Q., 2006. Bioelectronchemistry 69, 10–15.
Zhou, H., Gan, X., Liu, T., Yang, Q.L., Li, G.X., 2005. J. Biochem. Biophys. Methods 64, 38–45.
Zhou, Y.L., Hu, N.F., Zeng, Y.H., Rusling, J.F., 2002. Langmuir 18, 211–219.